Remaining useful life prediction and uncertainty quantification of proton exchange membrane fuel cell under variable load

Mathieu Bressel, Mickael Hilairet, Hissel Daniel, Belkacem Ould Bouamama

Remaining Useful Life Prediction and Uncertainty Quantification of Proton Exchange Membrane Fuel Cell Under Variable Load

Mathieu Bressel, Mickael Hilairet, Daniel Hissel,
and Belkacem Ould Bouamama

Abstract—Although, Proton Exchange Membrane Fuel Cell is a promising clean and efficient energy converter that can be used to power an entire building in electricity and heat in a combined manner, it suffers from a limited lifespan due to degradation mechanisms. As a consequence, in the past years researches have been conducted to estimate the State of Health and now the Remaining Useful Life in order to extend the life of such devices. However, the developed methods are unable to perform prognostics with an online uncertainty quantification due to the computational cost. This paper aims at tackling this issue by proposing an observer-based prognostic algorithm. An Extended Kalman Filter estimates the actual State of Health and the dynamic of the degradation with the associated uncertainty. An Inverse First Order Reliability Method is used to extrapolate the State of Health until a threshold is reached, for which the Remaining Useful Life is given with a 90% confidence interval. The global method is validated using a simulation model built from degradation data. Finally, the algorithm is tested on a data set coming from a long term experimental test on a 8-cell fuel cell stack subjected to a variable power profile.

Keywords—Remaining Useful Life, PEM Fuel Cell, Ex-tended Kalman Filter, Inverse First Order Reliability Method

I. Introduction

Since fossil energy resources are reducing, an energy transition is required. One of the major problem that transition imposes is the storage of the electricity which can be tackled by the use of hydrogen as an energy vector which produces electricity through a fuel cell [1]. Those electrochemical converters, including the Proton Exchange Membrane Fuel Cell (PEMFC), receive a growing interest from industrial and scientific community worldwide. Indeed, they have a wide range of applications. PEMFC is a promising internal combustion engine substitute for clean and efficient transportation applications, but also as a portable source of low power [2]. In addition, in a larger scale, fuel cells are capable of powering an entire building in electricity and heat in a combined manner (μ-CHP) [3]. However, those promising converters suffer from a limited lifetime due to mechanical and electrochemical degradation that avoid there widespread deployment. Those phenomena include corrosion of the carbon support, the catalyst particles ripening, the compression of the gas diffusion layer (GDL), and they are far from being fully understood [4]. The degradation also depends on the operating conditions which makes the prediction of the power loss difficult [5].

This is the reason why Prognostics and Health Management (PHM) of PEMFC is gaining awareness in the research field. It allows extending the life of this electrochemical converter due to monitoring [6], diagnosis [7], [8], prognostic [9], and corrective actions at a decision level. By selecting specific features from sensors, one can build indicators of the State of Heath (SoH) of a system and track their evolutions in order to predict the End of Life (EoL). Despite the fact that many applications of Remaining Useful Life (RUL) prediction of PEMFC can be found in the literature, none of the developed approaches are able to predict the RUL when an unknown variable profile of power is considered.

The prognostic activity aims at the development of a robust algorithm to estimate the State of Health and to forecast the future behavior of a system, but it should also be able to quantify the confidence of the prediction. This is the reason why, researches have been focused on uncertainty quantification for prognostics [10]. Since data driven and hybrid uncertainty quantification methods are mostly based on sampling (i.e. Monte Carlo simulation), they remain computationally expensive [11]. The confidence in RUL prediction can also be evaluated by analytical approaches such as First Order Reliability Methods (FORM) which are much faster to compute and can be possibly implemented in real time [12]. Those techniques have been extensively used in the past for material and structural reliability and start to be applied to electrochemical systems. Although giving the confidence in the RUL prediction is of great interest, only one paper addresses this issue for PEMFC prognostics by using a Particle Filter [13].

As a consequence, to tackle those limitations, the presented work contributes to the observer-based prognostics by predicting the RUL of a PEMFC subjected to an unknown μ-CHP profile and by estimating the inherent uncertainty using an Extended Kalman Filter (EKF) and the Inverse First Order Reliability Method (IFORM). The aim is to develop a robust algorithm that can be implementable in real time.

In the first section a brief description of the test bench and the performed test can be found. section 3 presents the methodology for SoH estimation and uncertainty quantification using an EKF. It also describes the IFORM algorithm which is then

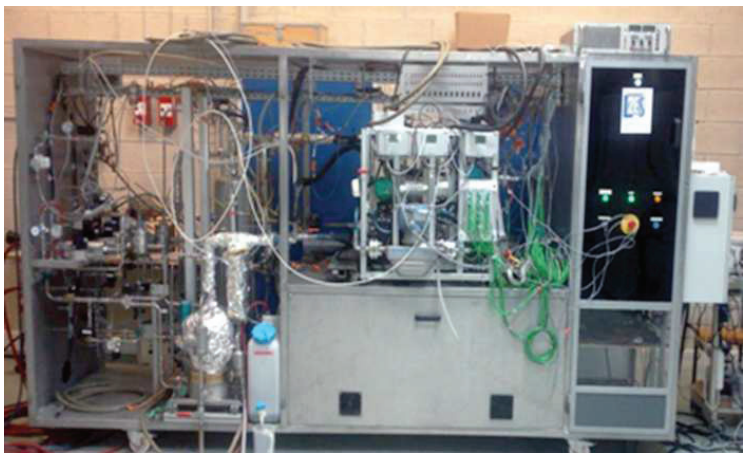

Fig. 1. 10kW in-lab test bench

Parameter	Value
Temperature	80°C
Anode and cathode stoichiometry ratios	1.5-2
Absolute pressure anode/cathode	1.5 bar
Relative humidity anode/cathode	50%
Nominal current density i_{nom}	0.45 $A.cm^{-2}$
Maximal current density i_{max}	0.77 $A.cm^{-2}$

Table 1: Operating conditions

applied to an 8-cell stack under a μ-CHP profile. A conclusion is provided in section 4.

II. Expiremental setup

To observe the aging, a 900 hours continuous experimental test is performed on an 8-cells fuel cell stack with a surface of 220 cm^2 provided by the French Atomic Energy and Alternative Energies Commission (CEA). A 10kW test bench (Fig. 1) regulates the temperature by mean of a cooling system while the stoichiometry and pressure are controlled continuously. Moreover, the test bench supplies the fuel cell in humidified hydrogen and air at the anode and cathode respectively. Tab. I shows the operating conditions.During the long time test, the PEMFC is subjected to a μ-CHP profile of current while the stack voltage is recorded with an hourly sample time as seen on Fig. 2. It aims at simulating the power required for a building along a year and follows the seasons:

- Winter: maximal current density i_{max} for about 250 hours
- Spring: 7 cycles of 24 hours between nominal current density i_{nom} and $\frac{i_{nom}}{2}$ followed by $\frac{i_{nom}}{2}$ until 500 hours
- Summer: $\frac{i_{nom}}{2}$ for 100 hours, followed by 9 cycles of 24 hours between $\frac{i_{nom}}{2}$ and no power demand until t=800 hours
- Autumn: $\frac{i_{nom}}{2}$ until the end of the test

In addition, periodically during the test, static and dynamic responses of the PEMFC are measured with polarization curves (as shown in Fig. 3) and Electrochemical Impedance Spectroscopy (EIS).

III. Prognostics of pem fuel cell

A. Generalities and method

Prognostics is the prediction of the remaining time before one or more failure modes appear avoiding a system to fulfill a given mission [14]. It is carried out in two steps: the actual SoH of the system is estimated, then the evolution of this SoH is forecasted until a threshold is reached. The time difference between the predicted EoL and the current time t_k is called the RUL.

$$RUL(t_k) = t_{EoL} - t_k \tag{1}$$

Several approaches have been developed to predict the RUL of PEMFC. They are divided into three categories [15]:

- Model based [16], [17], [18], [19]: the degradation is expressed using an analytical relation. Although the physical models are used when expert knowledge is available, it is often chosen to develop an empirical relation. The latter is the approach used in this paper.
- Data based [20], [21], [22]: the degradation is learned during the aging using tools from Artificial Intelligence. Despite this approach requires a huge amount of data, it is able to reproduce highly non-linear behaviors.
- Hybrid [23], [24], [25]: a model is used to improve the training compared to pure data based methods. However, implementing such algorithms in real time is difficult due to the computational cost.

Despite the fact that model based method gives auspicious results, it was never applied to estimate the RUL of a PEMFC under a variable load. Moreover from all the methods described above, only [13] addresses the issue of uncertainty quantification by mean of a Particle Filter which is challenging to implement online. As an extension of a previous work [26] and to tackle the computational limitation, the method presented in this paper (Fig. 4) allows a fast estimation of the

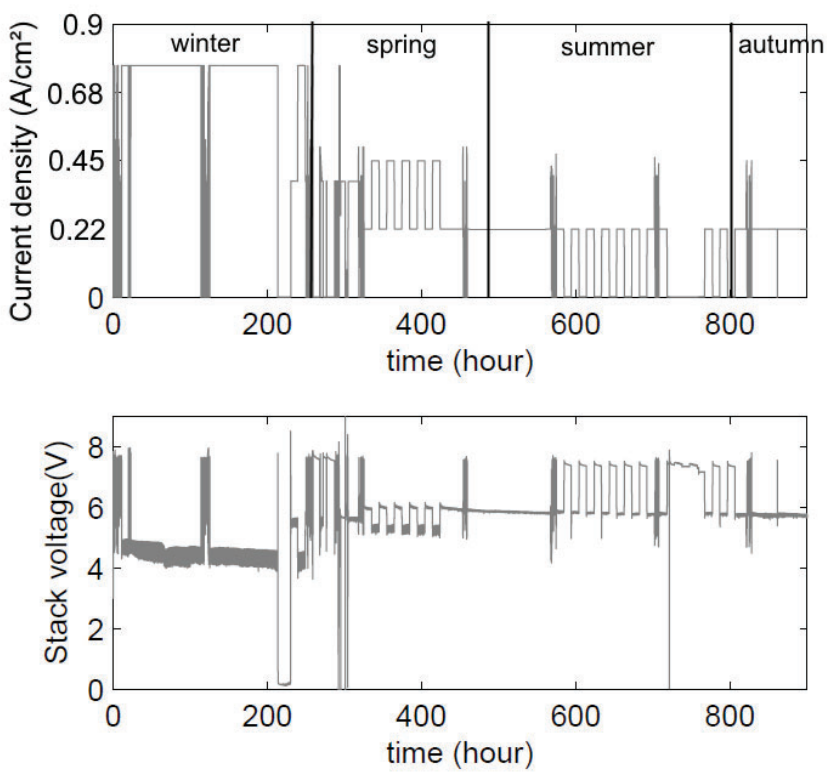

Fig. 2. Load current and recorded stack voltage

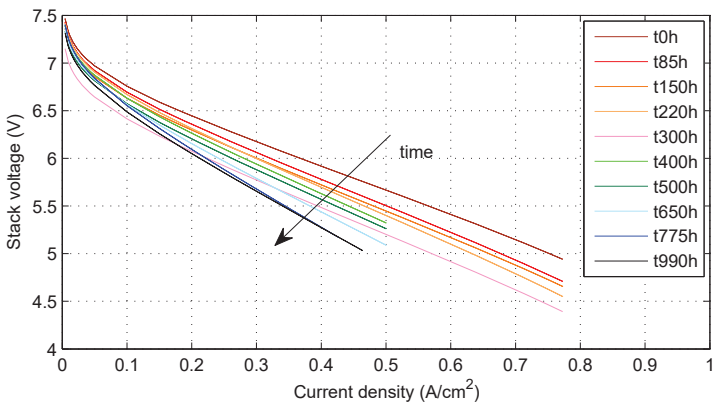

Fig. 3. Polarization curves during aging

SoH and RUL of a PEMFC under a variable load with uncertainty quantification. It consists of an offline analysis of the PEMFC electro-chemical parameters degradations. Precisely, a nonlinear optimization algorithm is applied to fit a model to the recorded polarization curves. The output of this algorithm is the evolution of the parameters of the model during the aging as presented in section 3.B, an empirical model of degradation is then built. Afterward, this model is used online with an observer to estimate the SoH and the uncertainty of the state at each sampling time (see section 3.C). Finally, considering the SoH estimation as a random variable, an IFORM is applied for the RUL and probability bounds estimation in section 3.D.

The uncertainty computed by the EKF has been widely used for assessing the accuracy of a state estimation [27], [28], [29]. Nevertheless, in the consulted literature dealing with EKF based prognostic, the setting of the filter for which the value of the uncertainty is strongly dependent, is usually not discussed. This issue might be solved using the Unscented Kalman Filter [16], [30] or an online estimation of the process covariance matrix for the EKF [31], [32].

As a novelty, the method presents the advantages of working for different operating conditions (of temperature, load and pressure) and for different PEMFC under the condition of having the initial polarization curve and thus does not require a lot of training comparing to data and hybrid based methods. Moreover, the EKF allows to compute the uncertainty of the estimates (due to the setting of the covariance matrices) and can be used online as discussed in the section 3.E.

B. Design of the degradation model

To study the effect of the aging on the electrochemical parameter's value, a Levenberg-Marquardt optimization algorithm extracts some parameters of the following equation on every polarization curve (see Fig. 3) :

$$V_{st} = n.\left(E_0 - A.T.ln\left(\frac{i}{i_0}\right) - R.i - B.T.ln\left(1 - \frac{i}{i_L}\right)\right) \quad (2)$$

with V_{st} the stack voltage, n is the number of cells of the stack, i the load current density, T the temperature, A the Tafel constant, and B the concentration constant. Since the voltage equation above is from a nonlinear nature, the Levenberg-Marquardt optimization method can only reach a local minimum. To overcome this issue, the algorithm is

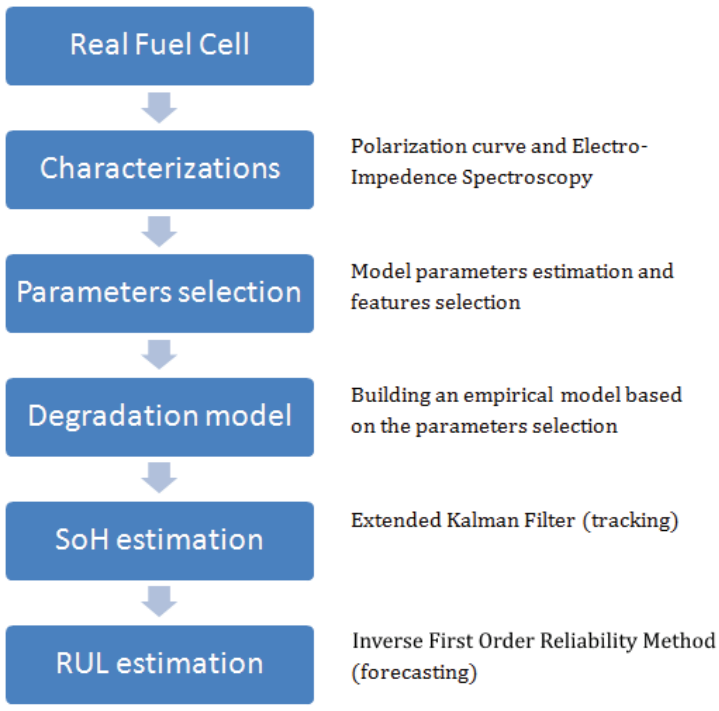

Fig. 4. Model-based prognostics methodology for PEMFC

initiated with standard values found in the literature [33], [34]. However, some optimization methods based on artificial intelligence are able to find the global minimum [35], [36]. For the sake of clarity, only the result of the model fitting for the first polarization curve is shown (see Fig. 5) for which the extracted parameters are:

- The Open Circuit Voltage (OCV) E_0 at nominal pressure and temperature
- The exchange current density i_0
- The overall resistance R (membranes, connectors, end plates, etc.)
- The limiting current density i_L

The OCV is dependent on the pressure following the Nernst law [37]. Nevertheless, the pressure inside the channels is kept constant due to the control unit and so does not affect the value of E_0. On this model fitting example, the Mean Average Percentage Error (MAPE) is equal to 0.6 %. This validated model allows to handle all the operating conditions specified in the test protocol of the section II. It is noted that other measurement method like the EIS allows to extract some parameters value (for instance the membrane conductivity). From the experimental data, the deviation of the chosen parameters through time with respect to the initial polarization curve is shown in Fig. 6.

Among them, the voltage E_0 and the exchange current i_0

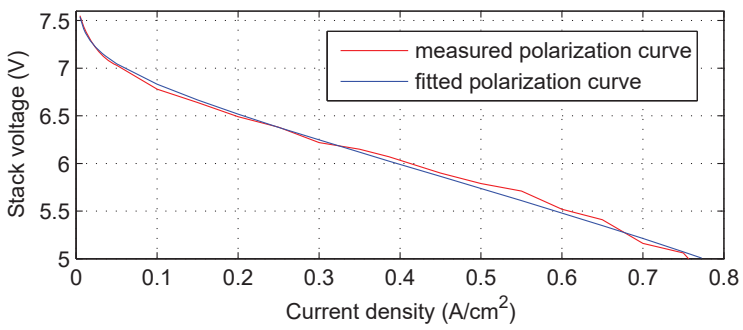

Fig. 5. Measured and fitted polarization curve

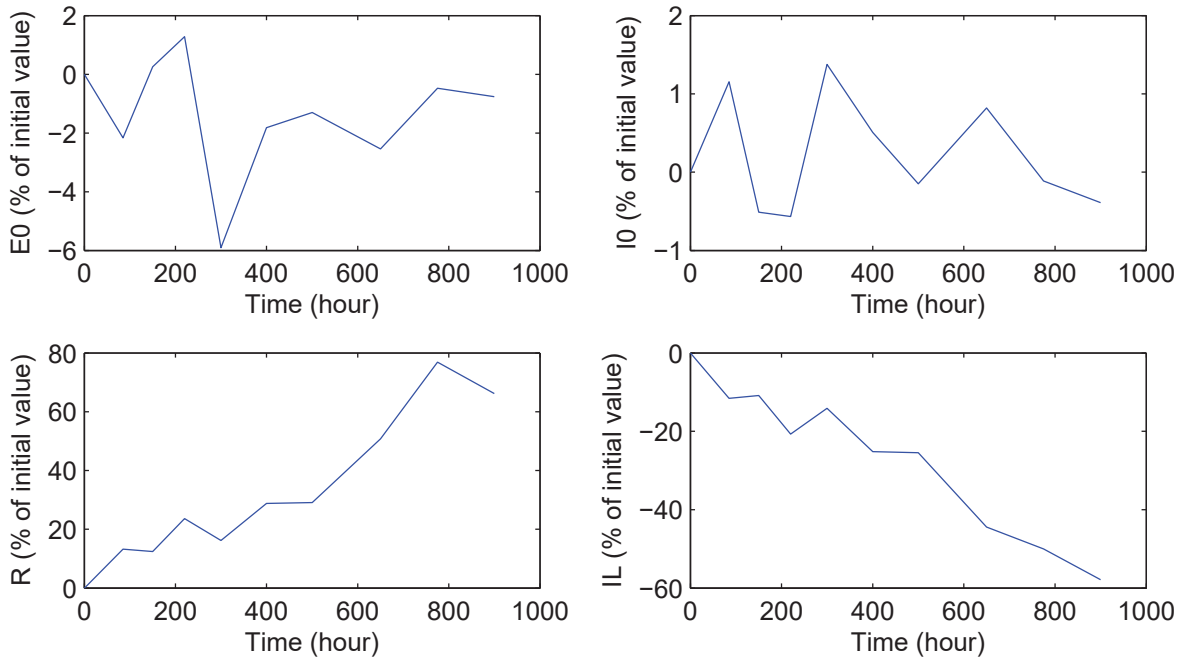

Fig. 6. Parameters deviation during aging

do not exhibit strong variations during the aging compared to the global resistance R and the limit current density i_L. One can conclude that the catalytic activity does not reduce through time and the volume of the channels remains the same (the pressure loss is not affected during aging) and thus those parameters are considered constant. On the contrary, the resistance value changes by more than 70% while the limit current density i_L decreases of 60%. This can be due to the dehydration or degradation of the polymer membrane, the corrosion of the plates or the corrosion of the catalyst support for the first [38]. The dehydration of the membrane, caused by a poor water management, provokes a higher ionic resistance and thus increase the loss by ohm effect locally. Moreover, the latter leads to the formation of pin hole and cracks which results in an higher gas crossover [39]. The decrease in the limit current density might be provoked by the compression of the GDL and the reduction of the electrochemical surface area (ECSA). One major cause is the migration of the catalyst particle (usually platinum) on the carbon support or their dissolution into the membrane which leads to the decreasing of the membrane conductivity [40]. Some details about the degradation mechanisms can be found in Pei et al [41].

From Fig. 6, it is clear that the speed of degradation is highly dependent on the current profile (e.g. cycles between nominal and Open Circuit Voltage [42]). Due to the fact that the power profile and the speed of degradation can not be expressed using physical laws, it is chosen to describe the aging with a linear equation. Moreover, by only measuring the stack voltage for a given current, it is impossible to separate the loss caused by the global resistance and the one caused by the limit current due to the non-observability of the state space system. This is the reason why, it is chosen to couple the deviation of the two parameters with a single variable $\alpha(t)$ which reflects the SoH:

$$R(t) = R_0(1+\alpha(t)), I_L(t) = I_{L0}(1-\alpha(t)), \tag{3}$$

$$\alpha(t) = \beta t \tag{4}$$

with β nearly constant.

C. Observer-based SoH estimation

1) Problem formulation: The joint estimation of the SoH α_k (indicator of degradation of the fuel cell) and the parameter β_k (speed of degradation) is based on the discrete nonlinear system:

$$x_{k+1} = Ax_{k|k} + w_k \tag{5}$$

$$y_k = g(x_k, u_k) + v_k \tag{6}$$

where $x_k = [\alpha_k \ \beta_k]^T$ is the state of the system, u_k represents the inputs (current load, temperature), y_k the output voltage, w_k and v_k are process and observation noises supposed Gaussian with zero mean and of variances Q and R respectively. Since the time constant for degradation is in the order of few hours, the thermal, electrical and hydraulic dynamics of the fuel cell are ignored. The stack voltage V_{st} seen in the previous section, expressed with regard to the SoH, is used as a measurement. In this joint state and parameter estimation problem, the transition matrix is:

$$A = \begin{bmatrix} 1 & T_s \\ 0 & 1 \end{bmatrix} \tag{7}$$

with T_s the sampling period of the observer and the regular discrete EKF is expressed as [43]:

Initialization

$x_{0|0} = E[x(t_0)]$

$P_{0|0} = Var[x(t_0)]$

Prediction

$x_{k|k-1} = Ax_{k-1|k-1}$

$P_{k|k-1} = AP_{k-1|k-1}A^T + Q$

Correction

$K_k = P_{k|k-1}H_k^T(H_kP_{k|k-1}H_k^T + R)^{-1}$

$with\ H_k = \frac{\partial g(x_k,u_k)}{\partial x_k}$

$$P_{k|k} = (I - K_k H_k) P_{k|k-1}$$
$$x_{k|k} = x_{k|k-1} + K_k (V_{stk} - g(x_k, u_k))$$

Despite the fact that the EKF is a linear algorithm, it has proven its effectiveness in estimation problems [44]. It is possible to estimate the non-linear SoH and its derivative for different current, temperature and speed of degradation β. Moreover, the EKF is able to give the uncertainty of the estimate through the covariance matrix of the estimates error P_k [45]. This motivated the choice of the EKF.

2) Setting and uncertainty of the state estimation: In the initialization of the EKF, the initial state vector $x_{0|0}$ and covariance of the state $P_{0|0}$ are required. Since the initial SoH and the speed of degradation are assumed unknown, $x_{0|0} = [0\ 0]^T$. The setting of the initial covariance matrix is performed by solving the algebraic Riccati equation in steady state when $P_{k|k} = P_{k-1|k-1}$:

$$A P_{k|k} A^T - P_{k|k} - A P_{k|k} H_k^T M H_k P_{k|k} A^T + Q = 0 \quad (8)$$

with $M = (H_k P_{k|k} H_k^T + R)^{-1}$ and H_k the observation matrix. Similar results can be obtained by running the EKF with a lower sample time for about a thousand iterations.

The output of the filter above is the optimal state estimation $x_k^\star$ given by the conditional probability density function:

$$p(x_k|y_k) \sim N(\hat{x}_k, P_k) \quad (9)$$

where $\hat{x}_k$ is the expected value and P_k is the covariance matrix of the estimation error defined by:

$$P_k = \begin{bmatrix} \sigma^2_{\alpha_k} & 0 \\ 0 & \sigma^2_{\beta_k} \end{bmatrix} \quad (10)$$

In the Kalman theory, P_k is a function of the process and measure noise variances which are ”usually” used as tuning variables. Nevertheless, to obtain the true uncertainty of the state estimate, Q and R have to be correctly set. The value of the measurement noise variance is obtained from computing the square of the standard deviation of the measured voltage seen in Fig. 2 [45]. Once that the test bench records the voltage with a different sampling rate $T_{s_{bench}}$, the discrete variance of measurement noise for the observer could be expressed as:

$$R_{T_s} \cong \frac{\sigma^2 . T_s}{T_{s_{bench}}} \quad (11)$$

Computing the analytical value of the process noise variance Q is a complicated task [32], it is therefore chosen to obtain it by minimizing a cost function J of the SoH obtained on a constant load aging long term test performed on the same test bench. The diagonal term Q_{11} is set to zero, once that α_k is the integral of β_k in the model.

$$Q = \begin{bmatrix} Q_{11} & 0 \\ 0 & Q_{22} \end{bmatrix} \quad (12)$$

$$J(Q_{22}) = \frac{1}{n} \sum_{k=0}^{n-1} (\hat{\alpha}_k - \alpha_k))^2 . k \quad (13)$$

with $\hat{\alpha}_k$ the estimation of the SoH at sample k, α_k the real SoH at sample k, and n is the number of samples of the test. Furthermore, since the algorithm has to give more accurate results in time, the quadratic function is multiplied by the sample number. If the EKF runs at a different sampling rate T_s than the test bench, the variance of the process noise could be evaluated as following:

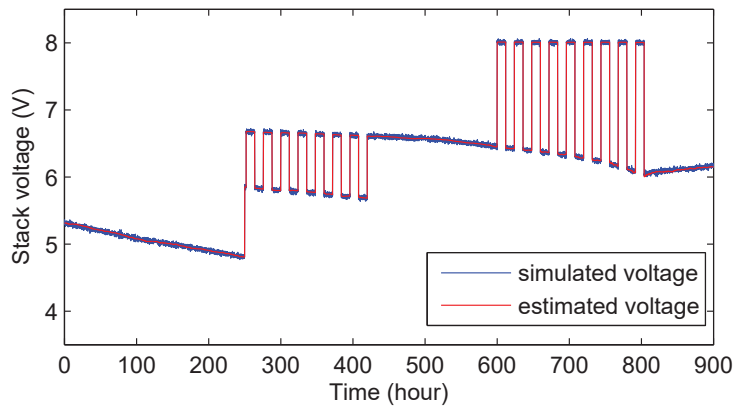

Fig. 7. Simulation and estimation of the stack voltage

$$Q_{T_s} \cong \frac{Q_{22} . T_s}{T_{s_{bench}}} \quad (14)$$

If Q is positive definite and the system is observable, then $P_{k|k}^{k \to \infty}$is unique, finite positive-semi-definite solution to the algebraic Riccati equation, independent of $P_{0|0}$ and the steady state EKF is asymptotically unbiased. With this setting of the noises, the diagonal terms of the covariance matrix P_k give the uncertainty on the State of Health and speed of degradation estimation [46].

3) Simulation results: To verify the effectiveness of the damage tracking algorithm, an aging fuel cell is simulated on Matlab-Simulink® using an Intel i5 Processor, 2.40GHz clock frequency and 4GB RAM. The current profile described in section 2 is used as the input of a PEMFC model where the parameters $R(t)$ and $I_L(t)$ evolve through time at different constant degradation rates. Fig. 7 shows the simulated voltage and its estimation by the EKF. The result of the estimation of the SoH $\alpha(t)$ and the speed of degradation $\beta(t)$ with the 99% probability bounds (3σ) are shown in Fig. 8. To evaluate the performance of this damage tracking algorithm, the Root Mean Square Error (RMSE) of the voltage, SoH and speed of degradation is computed (see Tab. II). The MAPE, which allows to evaluate the relative error, would be a better indicator. Nevertheless it can not be used for assessing the state estimation accuracy since α and β cross the zero-value.

Variable	RMSE
Voltage Vst	0.89%
State of Health α	0.23%
Speed of degradation β	0.018%

Table II. Accuracy of the EKF estimation

Although the load current varies, the voltage is accurately estimated by the EKF. Moreover, the SoH $\alpha(t)$ is correctly estimated with a high confidence. The EKF requires about 100 samples to converge and to estimate correctly the speed of degradation $\beta(t)$. To improve the convergence time, one

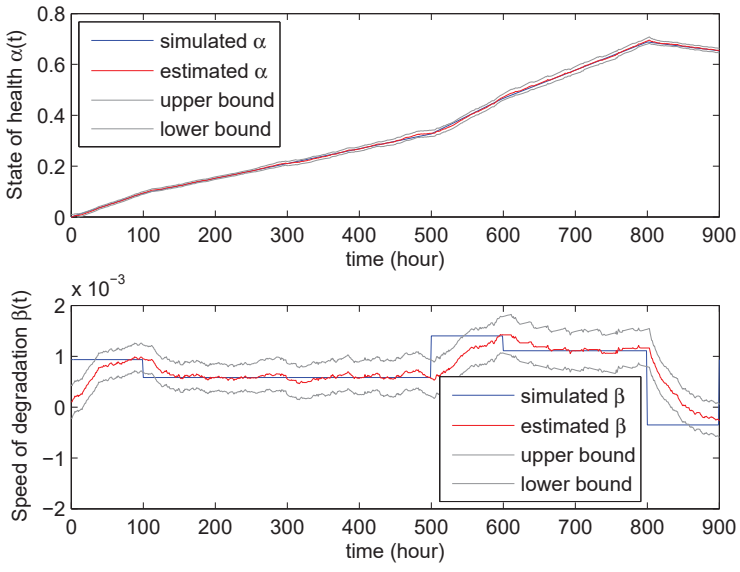

Fig. 8. Simulation and estimation of the SoH and speed of degradation

can run the algorithm at a higher sampling rate. As a result, the estimation will be more noisy and it should be avoided. This algorithm is able to estimate a new speed of degradation within 100 hours, which is well suited to a μ-CHP profile. Nevertheless, in transportation application, the PEMFC works with much faster dynamics of current what makes the prognostic more difficult. This issue will be subjected to future research.

D. IFORM for RUL estimation

1) IFORM algorithm: Most of the uncertainty quantification methods for the remaining useful life are based on Monte Carlo simulation which is computationally expensive. This is the reason why analytical method as the First Order Reliability Method is extensively used for effective failure probability calculation [47]. On the contrary, the IFORM is able to estimate the unknown parameters (e.g. RUL for prognostics) for a given failure probability level [48]. The IFORM algorithm requires a so called limit state function $g(u, y)$ which represents the limit between healthy state and failure mode in the random variable Standard Normalized Space (see Fig. 9). In this paper, the PEMFC is considered out of use when the SoH α reach a threshold α_{max}. As a consequence, the limit state function is expressed using the forecasted RUL which depends on the actual SoH and speed of degradation [49]:

$$RUL_k = \frac{\alpha_{max} - \alpha_k}{\beta_k . T_s} \tag{15}$$

$$g(u, y) = RUL_k(u) - y \tag{16}$$

where u is the vector of random state variable $x = [\alpha_k, \beta_k]^T$ expressed in the standard normalized space and y is the number of clock. The uncertain parameters have to satisfy the constraint:

$$P_f = \Phi(-\beta_{target}) \tag{17}$$

where the failure probability P_f is calculated using the Cumulative Distribution Function (CDF) of the reliability index β_{target} (not to confuse with the speed of degradation β_k). The later is defined as the distance between the origin and the Most Probable Point (MPP) in the standard normalized space:

$$||u|| = \beta_{target} \tag{18}$$

The IFORM algorithm aims at finding the MPP using numerical minimum search techniques satisfying the constraints for a given P_f (where $\beta_{target} = \Phi^{-1}(P_f)$). The iterative procedure follows the steps bellow:

1) The counter j is set to zero and an initial guess for the MPP is chosen $x^j = \{x_1^j, x_2^j\}$
2) The coordinates are transformed into normal space using the mean and variance from the EKF (μ_i and σ_i respectively):
$$u_i^j = \frac{x_i^j - \mu_i}{\sigma_i} \tag{19}$$
3) The gradient vector of the limit state function is computed:
$$a_i = \frac{\partial g}{\partial u_i} = \frac{\partial g}{\partial x_i} . \frac{\partial x_i}{\partial u_i} \tag{20}$$
4) The next point is computed using:
$$u^{j+1} = -\frac{a}{|a|} . \beta_{target} \tag{21}$$
5) x^{j+1} is computed by transforming back into the original space and the steps are repeated from 3 until the algorithm converges (usually in 4-5 iterations).

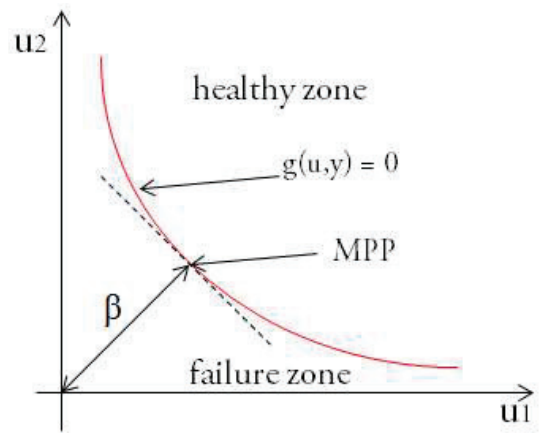

Fig. 9. Limit state function and Most Probable Point

Two criteria for the convergence must be satisfied (using tolerance δ_1 and δ_2):

- The MPP must lie in the limit state function:
$$|g(x^j) - y| \leq \delta_1 \tag{22}$$
- The coordinates of the point are nearly constant between two iterations:
$$|x^{j+1} - x^j| \leq \delta_2 \tag{23}$$

One can obtain probability bounds by repeating this algorithm for different P_f. For example, with $P_f = \{0.05, 0.5, 0.95\}$, the algorithm estimates the RUL and the 90% probability bounds. Details about the general methodology and computational considerations can be found in [50] and [12] respectively.

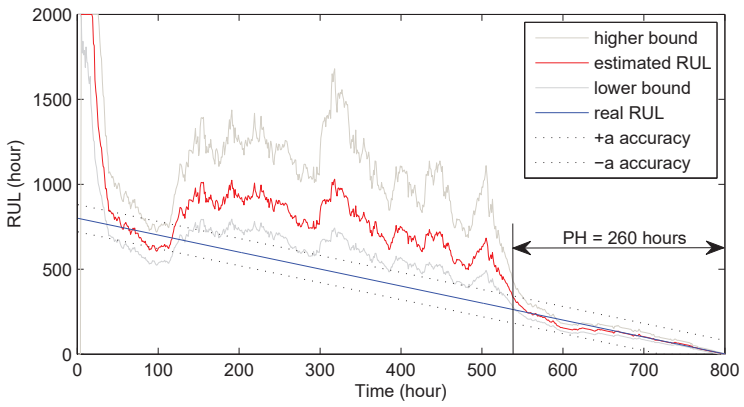

Fig. 10. RUL estimation with 90% probability bounds and PH metric

2) Simulation results: The estimation of the SoH, speed degradation and uncertainty by the EKF is given as input of the IFORM algorithm. The simulated PEMFC stack (see Fig. 7) has a maximum parameter deviation $\alpha_{max} = 70\%$ at $t_{EoL} = 800$ hours. This is considered as an indicator of good prediction even if the PEMFC can still operate afterward. Fig. 10 shows the estimation of the Remaining Useful Life with 90% probability bounds and the Prognostic Horizon metric (PH). The PH is the time for which the prediction is bounded in an allowable error a (i.e. $a = 0.1$ whether 80 hours). Fig. 11 shows the $a - \lambda$ performance metric. It quantifies the accuracy of the RUL prediction that must lies within a cone-shaped bounds (here $a = 0.15$) [51].

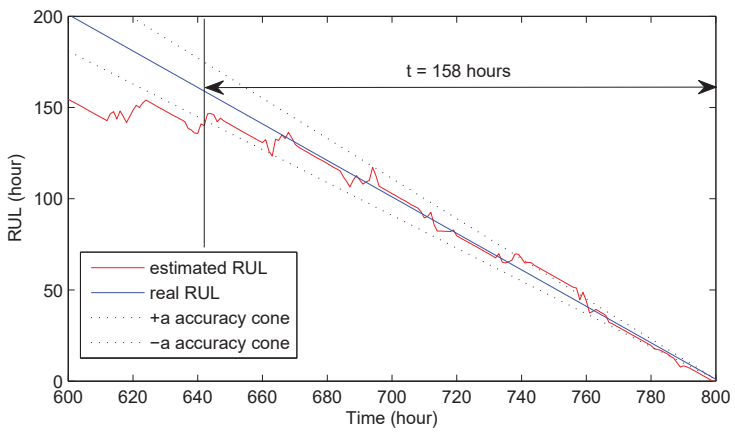

Fig. 11. RUL estimation and the $a - \lambda$ performance metric

Since, the Remaining Useful Life depends on the speed of degradation, one can notice different possible EoL (e.g. between $t = 200$ h and $t = 500$ h, the EoL seems to be extended to 900 hours). For instance, at $t = 200$h, the real EoL can not be forecasted once that the degradation model is not a function of the current profile. Moreover, since the EKF requires about 100 samples to converge, the RUL follows the same dynamic. In this simulation case, the PH is of about 260 hours (10.8 days) and the $a-\lambda$ is equal to 158 hours (6.6 days) which is enough time for planning a PEMFC replacement before failure. Moreover, the average Relative Accuracy $\overline{RA}$ is equal to 90% between $t = 540$ hours and the failure time t_{EoL}. It is noted that the uncertainty on the RUL estimation is also bounded by the PH metric at $t = 550$ hours and this can be used to compare with other uncertainty quantification of prediction methods even if the distribution is not a Gaussian [51]. This methodology gives auspicious results in the RUL

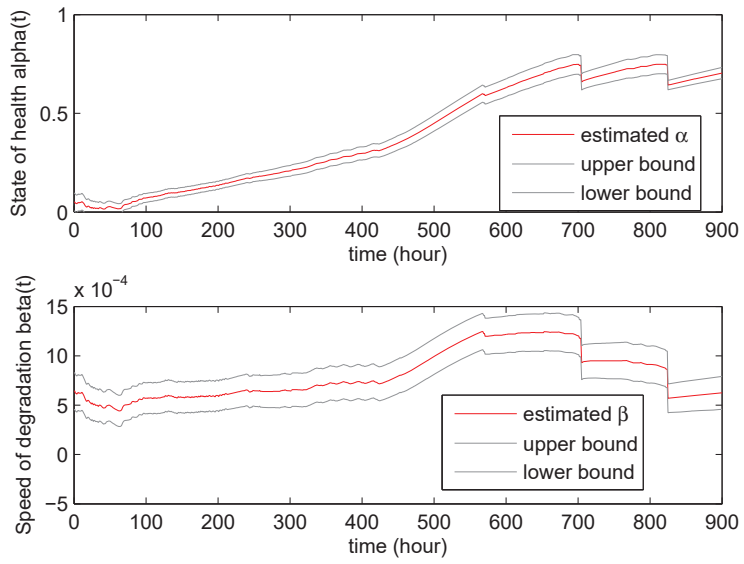

Fig. 12. α_k and β_k estimation with the 99% confidence interval

estimation with a high certainty after 550 hours and an high accuracy after 640 hours. The uncertainty decreases with time and the algorithm is able to re-evaluate the RUL when a change of speed of degradation is detected.

E. Experimental results and discussion

1) Results: The SoH and RUL estimation method presented above is applied to the 8-cell stack from section 2 (see Fig. 2). First, a polarization curve is performed where the initial set of parameters $\{E_0, I_0, R_0, I_{L0}\}$ is extracted using the Levenberg-Marquardt method (see section 3.B). Then, the EKF estimates hourly the SoH α_k and speed of degradation β_k as seen in Fig. 12.

One can notice that the estimation is affected when characterizations are performed. Indeed, a recovery effect happens on the stack voltage and leads to a better SoH. This phenomena can be due to the re-standardization of the conditions of temperature and by a proper evacuation of the liquid water in the PEMFC. Moreover, as expected from the parameters study of section 3.B, the current profile (i.e. the seasons) affects the speed of degradation which seems to be correctly tracked by the EKF. This leads to a re-evaluation of the RUL by the IFORM algorithm (see Fig. 13). This over and underestimation could be avoided with a physical model linking the speed of degradation and the operating conditions. The chosen

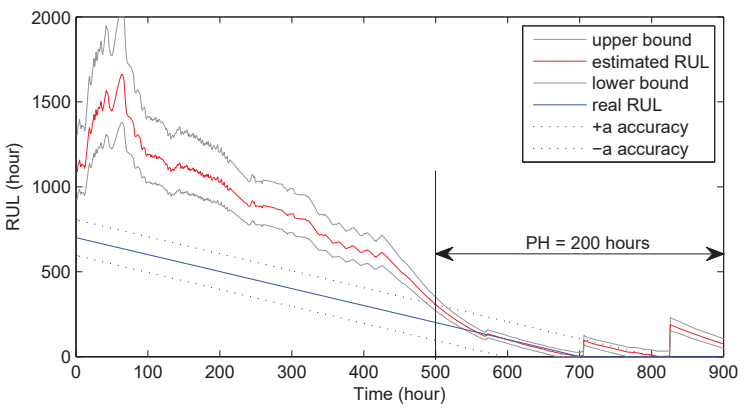

Fig. 13. RUL estimation with 90% probability bounds and PH metric

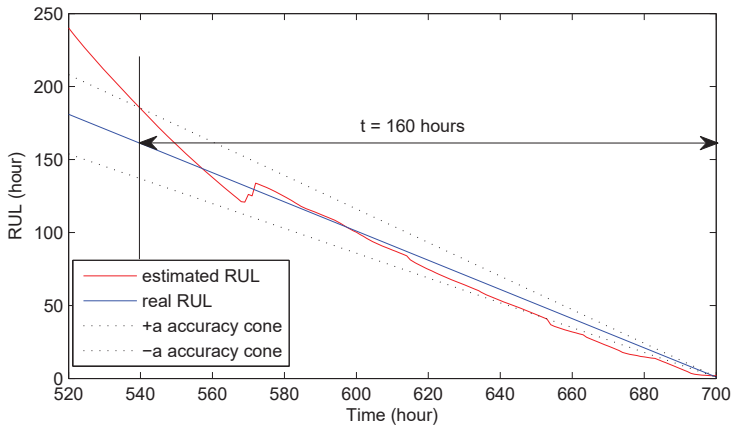

Fig. 14. RUL estimation and the a-λ performance metric

threshold for EoL of the PEMFC is a maximum parameter deviation $\alpha_{max} = 75\%$ which seems to be reached twice: $t = \{704, 820\}$. As a consequence, different EoL seems to appear:

- $100 < t < 400$, $t_{EoL} = 800$ h
- $570 < t < 700$, $t_{EoL} = 700$ h
- $704 < t < 820$, $t_{EoL} = 820$ h
- $820 < t$, $t_{EoL} = 950$ h

Similarly to the simulation case, several performance metrics are used. The real values of $\alpha(t)$ and $\beta(t)$ can not be obtained in-lab, thus it is impossible to evaluate the performance of the EKF on the state estimation. Nevertheless, one can assess the good estimation of the EKF with the RMSE of the stack voltage which is of about 9%. The PH (with a=0.1) is equal to 200 hours (8.3 days) as seen on Fig. 13. On Fig. 14, one can see that the $a - \lambda$ indicator (with a=0.15) is reached at $t = 160$ hours (6.7 days) and from $t = 540$ hours till t_{EoL} the $\overline{RA}$ is of about 87%. Likewise the simulation case, the uncertainty is bounded by the PH metric at $t = 520$ hours. The global method is able to estimate the RUL with a high confidence after 500 hours which is suited for a μ-CHP application.

2) Computational considerations: The total time required to run the EKF along this 900 hours data-set on an Intel i5 Processor, 2.40GHz clock frequency and 4GB RAM, is of about 1.2 seconds. When the IFORM algorithm is included, the total time is about 1.64 second. This can be explained by the fact that for each new sample, the IFORM algorithm takes in average 5 iterations before convergence. For the sake of comparison, a Particle Filter (PF) is used on the same data-set as an estimator with different settings. With N=2000 particles, the PF is giving better accuracy than EKF for the voltage estimation, nevertheless the total time is up to 4 hours and 28 minutes. For an estimation accuracy similar to the EKF (N=100 particles), the algorithm requires 5 min 45 seconds to compute the prediction. The accuracy and prediction time are resumed in Tab. III.

3) Discussion: The state estimation of the EKF is highly dependent on the setting of the covariance of the measurement and process noises. This issue is addressed in this paper. Nevertheless, the measurement noise is considered constant which is not the case in practice (i.e. the noise is greater at high current as seen in Fig. 2). The result of the algorithm could be

Estimator	$RMSE_V$	Total computational time
EKF and IFORM	9.02%	1.64s
PF (N=100)	9.03%	5min45s
PF (N=2000)	4.2%	4h28min

Table III. Performance comparison between PF and EKF

enhanced with an online standard deviation estimation of the measure noise [52] and a process noise chosen in accordance to this measure noise [53].

The method gives auspicious results despite an unknown variable speed of degradation and a recovery effect. Indeed, in real situations, the profile might not be fully known (i.e. lowering of the required power during mild winter) and the characterizations may not be performed periodically (absence of recovery). Moreover, the algorithm is able to provide the uncertainty of the SoH and RUL estimation with a low computational cost compared to the other uncertainty quantification methods. However, the time required by the EKF to converge makes the RUL estimation in vehicle applications challenging (due to higher dynamics) and it will be subject of further research.

IV. Conclusion

An observer-based prognostic algorithm for PEMFC is presented which is able to estimate the SoH and RUL with the inherent uncertainty. The aging of the PEMFC is predicted using an EKF and an empirical model of degradation which is based on a parameters analysis. The parameters of a static PEMFC model are obtained using a Levenberg-Marquardt optimization algorithm with a high accuracy for all the considered load current. The setting of the EKF is discussed which allows obtaining the state and the uncertainty of the estimates. These information are provided to an IFORM for fast and accurate RUL estimation and uncertainty quantification.

The presented method is able to give prognostic results for PEMFC under a μ-CHP current profile with an unknown speed of degradation, which would reflect better the yearly power demand of a real PEMFC in stationary applications. However, in vehicle applications, the required power follows higher dynamics, and so the RUL estimation algorithm has to be able to converge faster, or the method has to be adapted for the prediction of the average behavior in a specified time window. The RUL estimation and uncertainty quantification of PEMFC under a transportation cycle will be the subject of a future paper.

Acknowledgment

This work was supported by the project ANR PROPICE (ANR-12-PRGE-0001) and by the project Labex ACTION (ANR-11-LABX-01-0) both funded by the French National Research Agency.

References

[1] S. Vazquez, S. Lukic, E. Galvan, L. Franquelo, and J. Carrasco, "Energy storage systems for transport and grid applications," *IEEE Trans. Ind. Electron.*, vol. 57, no. 12, pp. 3881–3895, 2010.

[2] J. Fernandez-Moreno, G. Guelbenzu, A. Martin, M. Folgado, P. Ferreira-Aparicio, and A. Chaparro, "A portable system powered with hydrogen and one single air-breathing pem fuel cell," *Applied Energy*, vol. 109, pp. 60–66, 2013.

[3] S.-D. Oh, K.-Y. Kim, S.-B. Oh, and H.-Y. Kwak, "Optimal operation of a 1-kw pemfc-based micro-chp system for residential applications," *Applied Energy*, vol. 96, pp. 93–101, 2012.

[4] W. Schmittinger and A. Vahidi, "A review of the main parameters influencing long-term performance and durability of pem fuel cells," *JPS*, vol. 19, pp. 291–312, 2008.

[5] E. Breaz, F. Gao, A. Miraoui, and R. Tirnovan, "A short review of aging mechanism modeling of proton exchange membrane fuel cell in transportation applications," *IEEE IECON'14*, pp. 3941–3947, 2014.

[6] S. Yin, X. Li, H. Gao, and O. Kaynak, "Data-based techniques focused on modern industry: An overview," *IEEE Trans. Ind. Electron.*, vol. 62, no. 1, pp. 657–667, January 2015.

[7] Z. Li, R. Outbib, S. Giurgea, and D. Hissel, "Diagnosis for pemfc systems: A data- driven approach with the capabilities of online adaptation and novel fault detection," *IEEE Trans. Ind. Electron.*, vol. 62, no. 8, pp. 5164–5174, August 2015.

[8] S. Yin, S. Ding, X. Xie, and H. Luo, "A review on basic data-driven approaches for industrial process monitoring," *IEEE Trans. Ind. Electron.*, vol. 61, no. 11, pp. 6418–6428, November 2014.

[9] K. Javed, R. Gouriveau, N. Zerhouni, and P. Nectoux, "Enabling health monitoring approach based on vibration data for accurate prognostics," *IEEE Trans. Ind. Electron.*, vol. 62, no. 1, pp. 647–656, 2015.

[10] X. Si, "An adaptive prognostic approach via nonlinear degradation modelling: Application to battery data," *IEEE Trans. Ind. Electron.*, vol. 62, no. 8, pp. 5082–5096, August 2015.

[11] M. Orchard, P. Hevia-Kock, B. Zhang, and L. Tang, "Risk measures for particle-filtering-based state-of-charge prognosis in lithium-ion batteries," *IEEE Trans. Ind. Electron.*, vol. 60, no. 11, pp. 5260–5269, 2013.

[12] Y. Xiang and Y. Liu, "Efficient probabilistic methods for real-time fatigue damage prognosis," *Annual Conference of the PHM Society*, 2010.

[13] M. Jouin, R. Gouriveau, D. Hissel, M. Pera, and N. Zerhouni, "Prognostics of proton exchange membrane fuel cell stacks in a particle filtering framework including characterization disturbances and voltage recovery," *IEEE PHM conference*, pp. 1–6, 2014.

[14] ISO, "Iso 13381-1: Condition monitoring and diagnostics of machinery -prognostics - part1: General guidelines," 2004.

[15] M. S. Kan, A. C.C.Tan, and J. Mathew, "A review on prognostic techniques for non-stationary and non-linear rotating systems," *MSSP*, vol. 62, pp. 1–20, 2015.

[16] X. Zhang and P. Pisu, "An unscented kalman filter based approach for the health monitoring and prognostics of a polymer electrolyte membrane fuel cell," *Annual conference of the PHM*, 2012.

[17] H. Chen, P. Pei, and M. Song, "Lifetime prediction and the economic lifetime of proton exchange membrane fuel cells," *Applied Energy*, vol. 142, pp. 154–163, 2015.

[18] E. Lechartier, R. Gouriveau, M.-C. Pera, D. Hissel, and N. Zerhouni, "Static and dynamic modeling of a pemfc for prognostics purpose," *VPPC'14*, 2014.

[19] A. Hochstein, H.-I. Ahn, Y. T. Leung, and M. Denesuk, "Switching vector autoregressive models with higher-order regime dynamics," *IEEE PHM conference*, pp. 1–10, 2014.

[20] S. Morando, S. Jemei, R. Gouriveau, N. Zerhouni, and D. Hissel, "Fuel cells prognostics using echo state network," *IEEE IECON'13*, pp. 1632–1637, 2013.

[21] R. Silva, R. Gouriveau, S. Jemei, D. Hissel, L. Boulon, K. Agbossou, and N. Y. Steiner, "Proton exchange membrane fuel cell degradation prediction based on adaptive neuro fuzzy inference systems," *IJHE*, vol. 39, no. 21, pp. 11 128–11 144, 2014.

[22] K. Javed, R. Gouriveau, and N. Zerhouni, "Data-driven prognostics of proton exchange membrane fuel cell stack with constraint based summation-wavelet extreme learning machine," *FDFC'15, Toulouse - France*, pp. 1–8, 2015.

[23] M. Jouin, R. Gouriveau, D. Hissel, M. Pera, and N. Zerhouni, "Prognostics of pem fuel cell in a particle filtering framework," *IJHE*, vol. 39, pp. 481–494, 2014.

[24] J. K. Kimotho, T. Meyer, and W. Sextro, "Pem fuel cell prognostics using particle filter with model parameter adaptation," *IEEE PHM conference*, pp. 1–6, 2014.

[25] M. Jouin, R. Gouriveau, D. Hissel, M. Pera, and N. Zerhouni, "Prognostics of pem fuel cells under a combined heat and power profile," *IFAC INCOM'15*, vol. 48, no. 3, pp. 26–31, 2015.

[26] M. Bressel, M. Hilairet, D. Hissel, and B. Ould-Bouamama, "Extended Kalman filter for prognostic of proton exchange membrane fuel cell," *Applied Energy*, vol. 164, pp. 220–227, February 2015.

[27] A. P. Ompusunggu, J.-M. Papy, and S. Vandenplas, "Kalman filtering based prognostics for automatic transmission clutches," *IEEE Trans. Mechatron.*, 2015.

[28] P. Lall, R. Lowe, and K. Goebel, "Prognostics using kalman-filter models and metrics for risk assessment in bgas under shock and vibration loads," *Electronic Components and Technology Conference*, pp. 889–901, 2010.

[29] P. Lall, J. Wei, and K. Goebel, "Comparison of kalman-filter and extended kalman-filter for prognostics health management of electronics," *IEEE 13th ITHERM Conference*, pp. 1281–1292, 2012.

[30] M. Daigle, B. Saha, and K. Goebel, "A comparison of filter-based approaches for model-based prognostics," *IEEE Aerospace Conference*, 2012.

[31] V. A. Bavdekar, A. P. Deshpande, and S. C. Patwardhan, "Identification of process and measurement noise covariance for state and parameter estimation using extended kalman filter," *Journal of Process Control*, vol. 21, pp. 585–601, 2011.

[32] B. Feng, M. Fu, H. Ma, Y. Xia, and B. Wang, "Kalman filter with recursive covariance estimation sequentially estimating process noise covariance," *IEEE Trans. Ind. Electron.*, vol. 61, no. 11, pp. 6253–6263, 2014.

[33] J. Larminie and A. Dicks, *Fuel Cell Systems Explained*, 2nd ed. John Wiley & Sons, 2003.

[34] E. Laffly, M. Pera, and D. Hissel, "Polymer electrolyte membrane fuel cell modelling and parameters estimation for ageing consideration," *IEEE International Symposium on Ind. Electron.*, pp. 180–185, 2007.

[35] Q. Li, W. Chen, Y. Wang, S. Liu, and J. Jia, "Parameter identification for pem fuel-cell mechanism model based on effective informed adaptive particle swarm optimization," *IEEE Trans. Ind. Electron.*, vol. 58, no. 6, pp. 2410–2419, 2011.

[36] A. Askarzadeh and A. Rezazadeh, "An innovative global harmony search algorithm for parameter identification of a pem fuel cell model," *IEEE Trans. Ind. Electron.*, vol. 59, no. 9, pp. 3473–3480, 2011.

[37] M. Bressel, M. Hilairet, D. Hissel, and B. Ould-Bouamama, "Dynamical modeling of proton exchange membrane fuel cell and parameters identification," *FDFC'15, Toulouse - France*, 2015.

[38] J. Kim, J. Lee, and H. Cho, "Equivalent circuit modeling of pem fuel cell degradation combined with a lfrc," *IEEE Trans. Ind. Electron.*, vol. 60, no. 11, pp. 5086–5094, 2013.

[39] M. Inaba, T. Kinumoto, M. Kiriake, R. Umebayashi, A. Tasaka, and Z. Ogumib, "Gas crossover and membrane degradation in polymer electrolyte fuel cells," *Electrochimica Acta*, vol. 51, pp. 5746–5753, April 2006.

[40] J. Wu, X. Z. Yuan, J. J. Martin, H. Wang, J. Zhang, J. Shen, S. Wu, and W. Merida, "A review of pem fuel cell durability: Degradation mechanisms and mitigation strategies," *JPS*, vol. 184, pp. 104–119, June 2008.

[41] P. Pei and H. Chen, "Main factors affecting the lifetime of proton exchange membrane fuel cells in vehicle applications: A review," *Applied Energy*, vol. 125, pp. 60–75, 2014.

[42] S. Kundu, M. Fowler, L. Simon, and R. Abouatallah, "Reversible and irreversible degradation in fuel cells during open circuit voltage durability testing," *JPS*, vol. 182, pp. 254–258, 2008.

[43] A. P. Andrews and M. S. Grewal, *Kalman Filtering Theory and Practice Using MATLAB*, 2nd ed. Wiley, 2001.

[44] F. Auger, M. Hilairet, J. Guerrero, E. Monmasson, T. Orlowska-Kowalska, and S. Katsura, "Industrial applications of the Kalman filter: A review," *IEEE Trans. Ind. Electron.*, vol. 60, no. 12, pp. 5458–5471, 2013.

[45] J. R. Celaya, A. Saxena, and K. Goebel, "Uncertainty representation and interpretation in model-based prognostics algorithms based on kalman filter estimation," *Annual Conference of the PHM Society*, 2012.

[46] R. Singleton, E. Strangas, and S. Aviyente, "Extended kalman filtering for remaining-useful-life estimation of bearings," *IEEE Trans. Ind. Electron.*, vol. 62, no. 3, pp. 1781–1790, 2015.

[47] M. Hohenbichler, S. Gollwitzer, W. Kruse, and R. Rackwitz, "New light on first- and second- order reliability methods," *Structural Safety*, vol. 4, no. 4, pp. 267–284, 1987.

[48] S. Sankararaman and K. Goebel, "Remaining useful life estimation in prognostics: An uncertainty propagation problem," *Aerospace Conference 2013*, 2013.

[49] P. Lall, R. Lowe, and K. Goebel, "Prognostics health management of electronic systems under mechanical shock and vibration using kalman

filter models and metrics," *IEEE Trans. Ind. Electron.*, vol. 59, no. 11, pp. 4301–4314, 2012.
[50] S. Sankararaman, M. J. Daigle, and K. Goebel, "Uncertainty quantification in remaining useful life prediction using first-order reliability methods," *IEEE Trans. Rel.*, vol. 63, no. 2, pp. 603–619, 2014.
[51] A. Saxena, J. Celaya, B. Saha, S. Saha, and K. Goebel, "Metrics for offline evaluation of prognostic performance," *International Journal of PHM*, vol. 1, no. 1, pp. 1–20, 2010.
[52] K. Yuen, P. Liang, and S. Kuok, "Online estimation of noise parameters for kalman filter," *Structural Engineering & Mechanics*, vol. 47, no. 3, 2013.
[53] M. Nilsson, "Kalman filtering with unknown noise covariances," *Reglermte*, 2006.